



HAL
open science

Identification of an Arabidopsis Feruloyl-Coenzyme A Transferase Required for Suberin Synthesis

Isabel Molina, Yonghua Li-Beisson, Fred Beisson, John B Ohlrogge, Mike Pollard

► **To cite this version:**

Isabel Molina, Yonghua Li-Beisson, Fred Beisson, John B Ohlrogge, Mike Pollard. Identification of an Arabidopsis Feruloyl-Coenzyme A Transferase Required for Suberin Synthesis. *Plant Physiology*, 2009, 151 (3), pp.1317-1328. 10.1104/pp.109.144907 . hal-03380508

HAL Id: hal-03380508

<https://hal.science/hal-03380508>

Submitted on 15 Oct 2021

HAL is a multi-disciplinary open access archive for the deposit and dissemination of scientific research documents, whether they are published or not. The documents may come from teaching and research institutions in France or abroad, or from public or private research centers.

L'archive ouverte pluridisciplinaire **HAL**, est destinée au dépôt et à la diffusion de documents scientifiques de niveau recherche, publiés ou non, émanant des établissements d'enseignement et de recherche français ou étrangers, des laboratoires publics ou privés.

Identification of an Arabidopsis Feruloyl-Coenzyme A Transferase Required for Suberin Synthesis^{1[W][OA]}

Isabel Molina, Yonghua Li-Beisson², Fred Beisson², John B. Ohlrogge, and Mike Pollard*

Department of Plant Biology, Michigan State University, East Lansing, Michigan 48824

All plants produce suberin, a lipophilic barrier of the cell wall that controls water and solute fluxes and restricts pathogen infection. It is often described as a heteropolymer comprised of polyaliphatic and polyaromatic domains. Major monomers include ω -hydroxy and α,ω -dicarboxylic fatty acids, glycerol, and ferulate. No genes have yet been identified for the aromatic suberin pathway. Here we demonstrate that Arabidopsis (*Arabidopsis thaliana*) gene *AT5G41040*, a member of the BAHD family of acyltransferases, is essential for incorporation of ferulate into suberin. In Arabidopsis plants transformed with the *AT5G41040* promoter:YFP fusion, reporter expression is localized to cell layers undergoing suberization. Knockout mutants of *AT5G41040* show almost complete elimination of suberin-associated ester-linked ferulate. However, the classic lamellar structure of suberin in root periderm of *at5g41040* is not disrupted. The reduction in ferulate in *at5g41040*-knockout seeds is associated with an approximate stoichiometric decrease in aliphatic monomers containing ω -hydroxyl groups. Recombinant *AT5G41040p* catalyzed acyl transfer from feruloyl-coenzyme A to ω -hydroxyfatty acids and fatty alcohols, demonstrating that the gene encodes a feruloyl transferase. *CYP86B1*, a cytochrome P450 monooxygenase gene whose transcript levels correlate with *AT5G41040* expression, was also investigated. Knockouts and overexpression confirmed *CYP86B1* as an oxidase required for the biosynthesis of very-long-chain saturated α,ω -bifunctional aliphatic monomers in suberin. The seed suberin composition of *cyp86b1* knockout was surprisingly dominated by unsubstituted fatty acids that are incapable of polymeric linkages. Together, these results challenge our current view of suberin structure by questioning both the function of ester-linked ferulate as an essential component and the existence of an extended aliphatic polyester.

Suberin is a lipophilic extracellular barrier deposited on the inner side of the primary cell wall. It functions to control fluxes of water and solutes, to contribute to the strength of the cell wall, and to provide a barrier to pathogen movement (Kolattukudy, 2001; Nawrath, 2002). It is synthesized constitutively during development by a variety of internal and exposed plant tissues, and as a response to stresses and wounding (Kolattukudy, 2001; Schreiber et al., 2005). The role of suberin in controlling salt stress and permeability has recently been demonstrated in mutants compromised in its biosynthesis (Beisson et al., 2007; Höfer et al., 2008; Serra et al., 2009).

Suberin is often described as a heteropolymer comprised of polyaliphatic and polyaromatic (polyphenolic) domains, with embedded waxes. Monomers

released by transesterification include aliphatics such as fatty acids, ω -hydroxyfatty acids (OHFAs), α,ω -dicarboxylic acids (DCAs), and fatty alcohols, often with a significant proportion of very-long-chain saturates ($\geq C_{20}$), plus glycerol and *p*-hydroxycinnamic acids (mainly ferulate; Matzke and Riederer, 1991; Bernards, 2002; Graça and Santos, 2006; Franke and Schreiber, 2007; Pollard et al., 2008). The aromatic network is a hydroxycinnamate-derived polymer, primarily comprised of C-C and ether-linked ferulic acid, *N*-feruloyltyramine, cinnamic acid, *p*-coumaric acid, or caffeic acid (Bernards et al., 1995). Glycerol-containing aliphatic dimers and trimers have been isolated by partial depolymerization methods (Graça et al., 2002; Graça and Santos, 2006). These studies have also identified the esterification of ω -OHFAs to each other, to DCAs, and to ferulate. Hydroxycinnamate esters with fatty alcohols that are extractable with organic solvents have been identified in many natural product studies. However, partial depolymerization studies with suberin have shown that a large portion of the ferulate is esterified to the terminal hydroxy group of long- and very-long-chain ω -OHFAs (Graça and Pereira, 2000; Graça and Santos, 2006). Likewise, a 22-caffeoyloxy-docosanoyl glycerol has been isolated from cotton (*Gossypium hirsutum*) fiber waxes (Schmutz et al., 1994). In these cases an ω -hydroxylase must provide the aliphatic substrate for the hydroxycinnamoyl transferase. Suberin monomer compositions have been described for Arabidopsis (*Arabidopsis thaliana*) tissues (Franke et al., 2005; Molina et al., 2006,

¹ This work was supported by the U.S. Department of Agriculture (grant no. 2005-35318-15419) and the National Science Foundation (grant no. MCB-0615563).

² Present address: Unité Mixte de Recherche 5200, Centre National de la Recherche Scientifique/University of Bordeaux, F-33076 Bordeaux, France.

* Corresponding author; e-mail pollard9@msu.edu.

The author responsible for distribution of materials integral to the findings presented in this article in accordance with the policy described in the Instructions for Authors (www.plantphysiol.org) is: Mike Pollard (pollard9@msu.edu).

[W] The online version of this article contains Web-only data.

[OA] Open Access articles can be viewed online without a subscription.

www.plantphysiol.org/cgi/doi/10.1104/pp.109.144907

2008), as have the alkyl hydroxycinnamate esters present in Arabidopsis root periderm (Li et al., 2007b).

Suberin deposition requires synthesis and assembly of metabolites from both the phenylpropanoid and acyl lipid pathways. The first genes affecting Arabidopsis aliphatic suberin and suberin-associated wax composition have been identified. These include the glycerol-3-P acyltransferase GPAT5 (Beisson et al., 2007; Li et al., 2007b) and an orthologous pair of cytochrome P450 ω -hydroxylases, CYP86A1 and CYP86A33 (Li et al., 2007a; Höfer et al., 2008; Serra et al., 2009). However, knockout mutants of these cytochrome P450 genes do not reduce the levels of ω -oxidized very-long-chain suberin monomers, so additional cytochrome P450 genes are required for this function. Here, we provide overlapping and additional information to the recent report that the P450 CYP86B1 (AT5G23190) is required for the synthesis of saturated very-long-chain α,ω -bifunctional monomers (Compagnon et al., 2009). In addition, although feruloyl transferase activity toward ω -OHFAs has been demonstrated in plant extracts (Lotfy et al., 1994, 1996), no genes encoding proteins with this function have been identified thus far. We describe an Arabidopsis gene (AT5G41040) that encodes such a feruloyl transferase, which we have named *ALIPHATIC SUBERIN FERULOYL TRANSFERASE* (*ASFT*). It is a member of the BAHD family of acyltransferases (St Pierre and De Luca, 2000; D'Auria, 2006), so named according to a letter from each of the first four biochemically characterized enzymes of the family, benzyl alcohol acetyltransferase, anthocynain-*O*-hydroxycinnamoyltransferase, anthranilate-*N*-hydroxycinnamoyl/benzoyltransferase, and deacetylvinidoline 4-*O*-acetyltransferase.

As suberin is an insoluble heteropolymer localized within the plant cell wall, solving its structure has been a challenging problem. When observed by transmission electron microscopy (TEM), suberin frequently exhibits a lamellar structure of alternating light and dark bands. Also, at least for wound-induced potato (*Solanum tuberosum*) periderm, the bulk of the phenolics appear to be deposited before the aliphatics (Lulai and Corsini, 1998; Yang and Bernards, 2007). Most of these phenolics are oxidatively cross linked (Bernards et al., 1995) and will not yield monomers by polyester depolymerization methods. Models for suberin structure of potato periderm (Bernards, 2002) or cork (*Quercus suber*; Graça and Santos, 2007), based as they are on earlier iterations (Kolattukudy, 1981), show some divergence, but agree that the electron-translucent bands are aliphatic rich and that there is an aliphatic polyester. The thickness of this layer coincides with the length of the carbon chain of the aliphatic monomers (Schmutz et al., 1996). Components of the opaque bands, which appear to vary considerably in thickness, may include glycerol, phenolics, and possibly aliphatics. In models of both potato and cork suberin oxidative cross linking of ferulic acid provides a covalent link between suberin

polyaromatic and polyaliphatic domains. The compositions of mutants can provide new perspectives on structural models. Our results with both BAHD and P450 genes suggest that, at least for seed suberin, two facets of proposed suberin structures, namely esterified ferulate as a linker between the aliphatic and aromatic domains, and the idea of an extended aliphatic polyester domain, will need to be carefully reexamined.

RESULTS

BAHD and *CYP86B1* Genes Correlated with the Expression of Suberin-Associated Genes

The recent identification of two Arabidopsis genes, *GPAT5* and *CYP86A1*, with confirmed roles in suberin biosynthesis provided an opportunity to apply transcript coreponse analysis to identify additional suberin-associated genes under common or related transcriptional control. These genes encode the acyltransferase GPAT5 (Beisson et al., 2007) and the cytochrome P450 monooxygenase CYP86A1, a fatty acyl ω -hydroxylase (Li et al., 2007a; Höfer et al., 2008). Using these two genes as the bait set, correlation analysis of gene expression across all microarray data sets (Wei et al., 2006) identified a number of other genes with a strong correlation (Supplemental Table S1), including two members of the BAHD gene family, *AT5G41040* (*ASFT*) and *AT5G63560*. Furthermore, the homolog of *ASFT* is among the list of genes that are both highly specific and highly expressed in cork phellem (Soler et al., 2007). The BAHD gene family is a large family of acyltransferases with 61 members in Arabidopsis (St Pierre and De Luca, 2000; D'Auria, 2006). To date all studied members of this family utilize relatively hydrophilic acyl-CoAs, including hydroxycinnamoyl-CoAs, as acyl donors in natural product synthesis. The purification of a tobacco (*Nicotiana tabacum*) feruloyl transferase activity utilizing 16-hydroxypalmitate as acyl acceptor clearly showed the activity to be soluble (Lotfy et al., 1996), consistent with expectations for enzymes of the BAHD family. An analysis of the Arabidopsis BAHD family shows 11 clades (Supplemental Fig. S1). Three genes cluster together in clade H, namely *ASFT*, *AT5G63560*, and *AT3G48720*. This clustering is also noted in a recent phylogenetic analysis of BAHD proteins (Yu et al., 2009). While expression of both *ASFT* and *AT5G63560* correlate highly with the suberin bait set, expression of *AT3G48720* shows correlations with some genes of cutin biosynthesis. In summary, the expression data, combined with phylogenetic analysis and known general biochemical function made *AT5G41040* (*ASFT*) and *AT5G63560* strong candidates for a putative feruloyl transferase. In fact, *AT5G41040* is clearly a feruloyl transferase that controls almost all the ester-linked ferulate deposition, and is described here. The function of *AT5G63560* is still under investigation in

our lab. Because ferulate is likely to be esterified to very-long-chain ω -hydroxy fatty acids we also investigated an uncharacterized P450 gene, *CYP86B1* (*AT5G23190*), that was shown to be correlated with the suberin bait set (Supplemental Table S1; see below).

***ASFT* Is Expressed in Tissues of Seeds and Roots Where Suberization Occurs**

Suberin is found in periderm of stems and of underground organs. In primary roots, it is present in endodermal, rhizodermal, and hypodermal cells (Ma and Peterson, 2003). It also may be deposited in seed coat layers during seed development (Espelie et al., 1980; Molina et al., 2008). To investigate the tissue specificity and temporal pattern of expression of *ASFT* in detail, transcriptional fusions were made by adding the 2-kb putative promoter sequence of *ASFT* upstream of the *eYFP* gene, which encodes the yellow fluorescent reporter protein, and this fusion was used to produce stable transgenic Arabidopsis plants. Analysis by confocal laser-scanning microscopy (CLSM; Fig. 1) revealed gene expression in seed coats (Fig. 1, A–C) and roots (Fig. 1, D and E), but not in other plant parts. These results agree with and extend to the cellular level microarray data for *ASFT* from the

AtGenExpress project (Schmid et al., 2005). In seed coats, *eYFP* was detected in the inner layer of the outer integument (*oi1*) beneath the *oi2* (columellae) layer, at the beginning of the desiccation stage (Fig. 1, A–C). This observation is reminiscent of *GPAT5* promoter activity shown both with YFP (Molina et al., 2008) and GUS (Beisson et al., 2007) reporters, and to *CYP86A1* expression (data not shown). As desiccation proceeds, strong *ASFT* expression was also observed at the chalazal region (Fig. 1A), as described for *GPAT5* expression. In primary roots of seedlings grown in agar for 1 or 2 weeks, YFP fluorescence was observed in the endodermis (Fig. 1, D and E); in 4- to 6-week-old seedlings, YFP expression was detected in the periderm of the zone of the roots that underwent secondary thickening (Fig. 1F), and in the endodermis of root parts in primary developmental stage. *CYP86A1* has been shown to have a similar pattern of root expression (Höfer et al., 2008). Taken together, our observations indicate that *ASFT* is expressed in tissues and cell layers where suberin is being deposited.

***ASFT* Is Required for the Deposition of Ferulate Monomer in Suberin**

Two mutant alleles of *ASFT* were selected by PCR screening of genomic DNA from segregating popula-

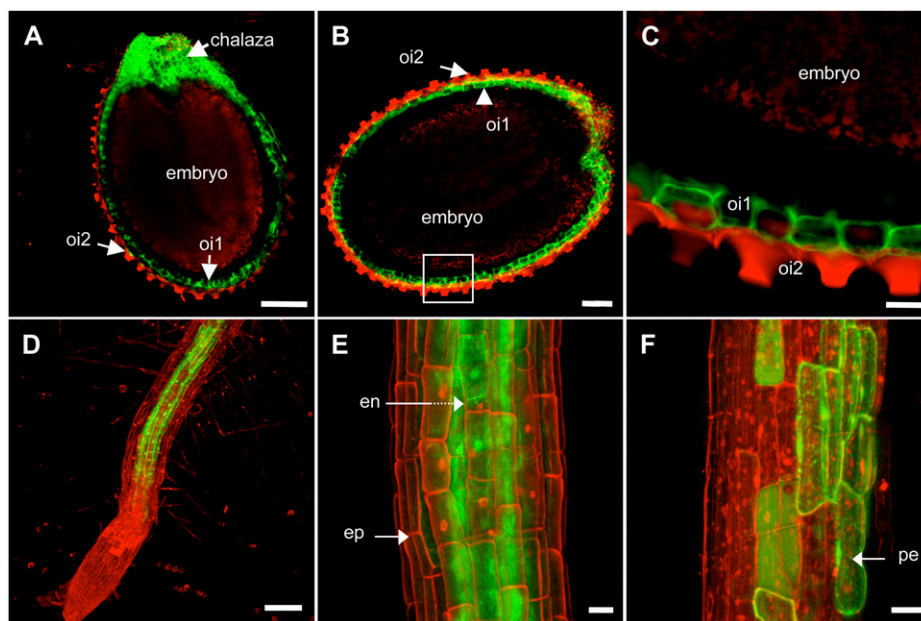


Figure 1. Analysis of *ASFT* promoter activity in Arabidopsis developing seeds and roots. Living transgenic seeds and roots from plants transformed with *Pro_{ASFT}::eYFP* were analyzed by CLSM. A and B, Confocal sections of transgenic seeds entering desiccation stage show YFP expression in the outer integument 1 (*oi1*) and the chalazal region of the seed coat. C, Magnification of the seed section shown in B. The YFP expression is beneath the columellae of the mucilage cells (*oi2*). D and E, Extended focus fluorescence images compiled from 26 (D) and 12 (E) optical sections of 2-week-old transgenic roots. YFP expression is localized to the endodermis. F, Extended focus fluorescence image compiled from 11 optical sections of a 5-week-old transgenic root showing YFP fluorescence in peridermal cells. Red fluorescence in the embryo corresponds to chlorophyll; red fluorescence in seed coat columellae and root cell walls is produced by propidium iodide dye. Scale bar = 100 μ m (A and D), 50 μ m (B), 20 μ m (C, E, and F). en, Endodermis; ep, epidermis; pe, peridermis.

tions of T-DNA insertion lines. These are designated *asft-1* (SALK_048898) and *asft-2* (SALK_017725; Supplemental Fig. S2A). Since this gene is expressed in roots and seeds, but its expression is negligible in other organs, mRNA from *asft-1*, *asft-2*, and wild-type roots was isolated and subjected to reverse transcription (RT)-PCR. No transcripts of this gene were present in the mutant roots, confirming these lines carry null mutations (Supplemental Fig. S2B).

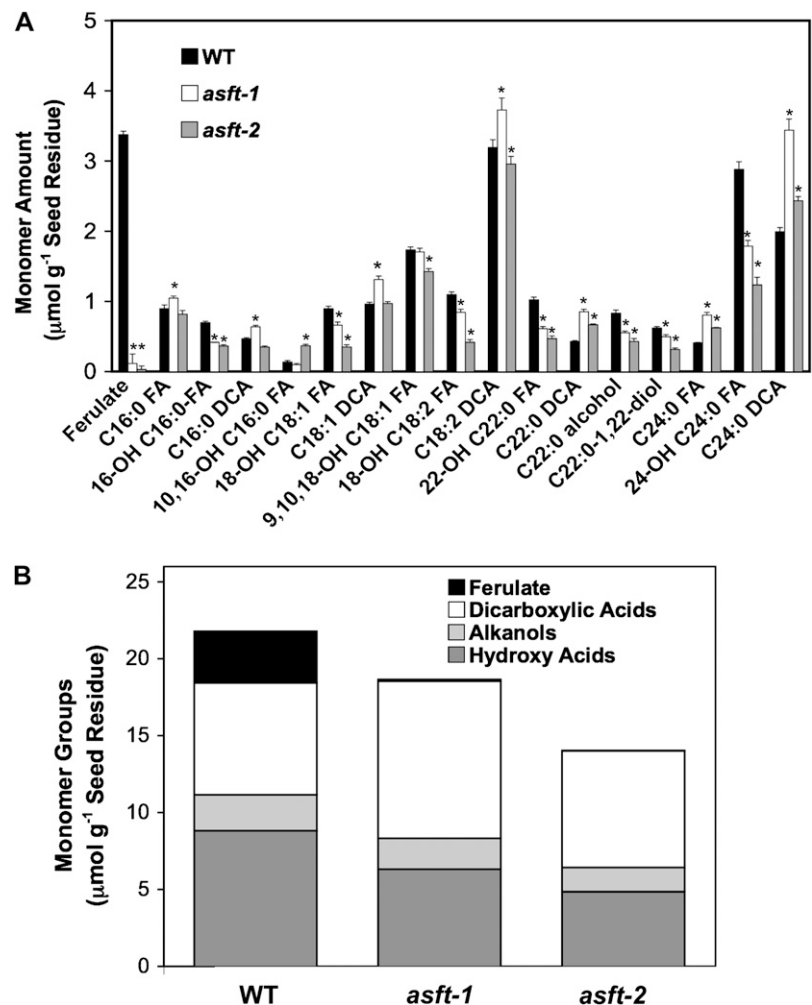
Wild-type and mutant plants grown side by side showed similar phenotypes. Monomers released by transesterification of delipidated seed residues (Fig. 2) revealed an almost complete loss of ferulate in seeds of both knockout alleles. An additional important observation when comparing *asft* mutants against wild type was that the reduction in ferulate of $1.55 \mu\text{mol g}^{-1}$ seeds for each allele was accompanied by a similar reduction in hydroxy-containing monomers, namely $1.35 \mu\text{mol g}^{-1}$ seeds in *asft-1* and $2.25 \mu\text{mol g}^{-1}$ seeds in *asft-2*. This observation suggests an approximate stoichiometric correlation between the losses of these two components. A substantial part of the reduction in aliphatics comes from C22 and C24 ω -OHFAs. In addition, a compensatory 50% increase in DCAs was

observed for *asft-1*. Thus the total aliphatic monomer content in the *asft-1* allele was the same as wild type ($8.89 \mu\text{mol g}^{-1}$ seeds), and reduced only by 10% in *asft-2* (Fig. 2B). Analysis of lipid polyesters in roots of 7-week-old plants (Supplemental Fig. S3) indicated that the ferulate amount is also greatly reduced in root suberin monomers released by transesterification. However, ferulate represents only 3% (w/w) of total root lipid polyester monomers. Aliphatic monomers containing a primary hydroxyl group did not appear to give a commensurate reduction, as in seeds, but minor changes in monomer levels may be masked by the higher variation usually observed in root polyester analysis.

The Deposition of Alkyl Hydroxycinnamate Esters of Suberin-Associated Waxes Is Not Altered in *asft* Roots

Endogenous waxes that are extracted by rapid chloroform dipping of roots contain alkyl trans-hydroxycinnamate esters, predominantly of coumarate and caffeate, with ferulate in lesser proportion (Li et al., 2007b). The alkyl groups are C18 to C22 saturated 1-alkanols. The relative amount of individual root wax

Figure 2. Comparison of lipid polyester monomer composition for wild-type (WT) and *asft* seeds. A, Individual monomers. Means of triplicate determinations and SD are indicated. Asterisks denote a significant difference from wild type (*t* test, two-sided $P < 0.05$). B, Total monomer amounts, with monomers grouped in four classes.



compounds in the *asft* mutants was indistinguishable from wild type (Fig. 3). This result indicated that the synthesis of alkyl ferulates, and more generally of alkyl hydroxycinnamate esters, is not affected in root suberin waxes of the knockouts. By comparison, the suberin-associated acyltransferase GPAT5 has been shown to participate in the deposition of both suberin waxes and polyester, indicating a biosynthetic overlap between extractable and insoluble components of suberin (Li et al., 2007b). Expression of *AT5G41040* under the control of its native or 35S promoters also produced no change in the composition of the root waxes (data not shown). Thus we expect that another BAHD enzyme, and possibly *AT5G63560*, might have a different specificity and be largely responsible for suberin wax formation in the root periderm. This hypothesis remains to be tested.

Loss of Ferulate Monomer Does Not Affect Suberin Lamellar Structure of Root Periderm Cells

Models describing the lamellar structure of suberin require esterified ferulate to covalently link aliphatic polyesters to the cross-linked aromatic domain(s) (Bernards, 2002; Graça and Santos, 2007). Because the chemical phenotype of *asft* is loss of ferulate, we investigated whether this loss would cause a change in the characteristic lamellar structure of suberin observed by TEM. Roots were chosen over seeds for ultrastructural analysis because Arabidopsis seeds are very small and in our hands their highly compacted seed coats made sample preparation problematic for TEM analysis and subsequent image interpretation. Arabidopsis root suberin presents the characteristic lamellar distribution (Franke et al., 2005) described in other species. Root ultrastructure was analyzed in *asft-1* and *asft-2* knockout mutants and, as a control, in *cyp86a1* knockout mutants. As noted earlier, *CYP86A1* is a suberin-associated P450 gene (Li et al., 2007a; Höfer et al., 2008). Its knockout shows a strong reduction in aliphatic suberin monomer amount, but a

relatively small reduction in ferulate. However, TEM identifies a strong perturbation in suberin structure for *cyp86a1* (Supplemental Fig. S4), also observed in the periderm of potato RNA interference lines where the homologous gene has been silenced (Serra et al., 2009). Figure 4 shows the results obtained for thin sections from 6-week-old *asft-1* roots. Surprisingly, no changes were observed in the fine structure of suberin deposited in periderm cells of this mutant (Fig. 4B), compared to wild type (Fig. 4A). This observation implies that the ferulate released by transmethylation does not contribute to the TEM-observable ultrastructure of wild-type root periderm suberin.

Recombinant ASFTp Functions as a Feruloyl Transferase

To determine the enzyme reaction catalyzed by ASFT, cell-free extracts of the recombinant protein expressed in *Escherichia coli* were used in enzyme assays to test for feruloyl transferase activity. Feruloyl-CoA was generated in situ by adding a recombinant tobacco 4-coumarate:coenzyme A ligase (Beuerle and Pichersky, 2002) plus ferulate, ATP, and CoASH to the reaction mixture. Primary alcohols of various chain lengths (C12–C18) and 15-hydroxypentadecanoic acid methyl ester were tested as acyl acceptors. Chloroform-soluble products were analyzed by gas chromatography-mass spectrometry (GC-MS). Figure 5 illustrates that the ASFTp catalyzes the formation of hexadecyl ferulate ester. The product peak at 38.5 min was only present when all the assay components were added (Fig. 5). In particular, the lack of any activity when either CoASH, ATP, or the 4-coumarate:coenzyme A ligase was omitted from the assay implies that the acyl donor for the reaction is indeed feruloyl-CoA. The corresponding electron impact (EI) spectrum showed the expected molecular ion of the silylated derivative (mass-to-charge ratio [*m/z*] = 490), plus diagnostic ions derived from the feruloyloxy group at *m/z* = 266, 265, and 249 (Fig. 5, inset). The ferulate ester was also formed using 15-hydroxypentadecanoic acid

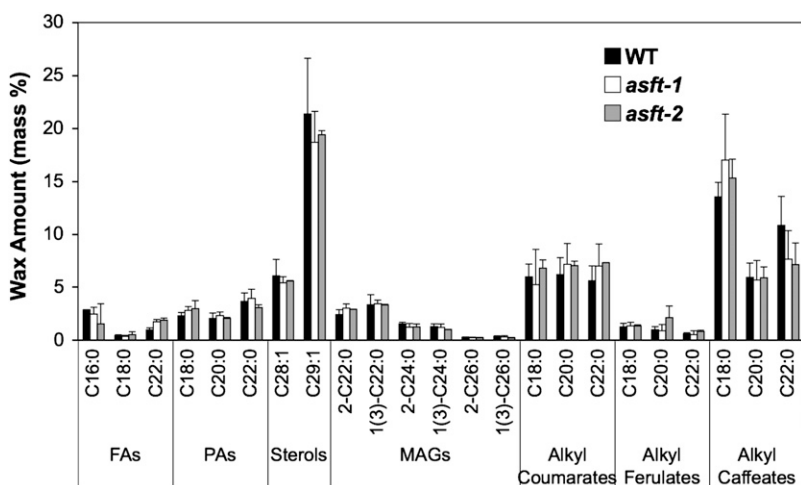


Figure 3. Root wax composition of wild-type (WT) and *asft* mutants. Composition of chloroform-extracted root waxes, expressed as mass % respect to total monomer amounts for each line. Means of triplicate determinations and *sd* are indicated. FAs, Free fatty acids; MAGs, monoacylglycerols; PAs, primary alcohols.

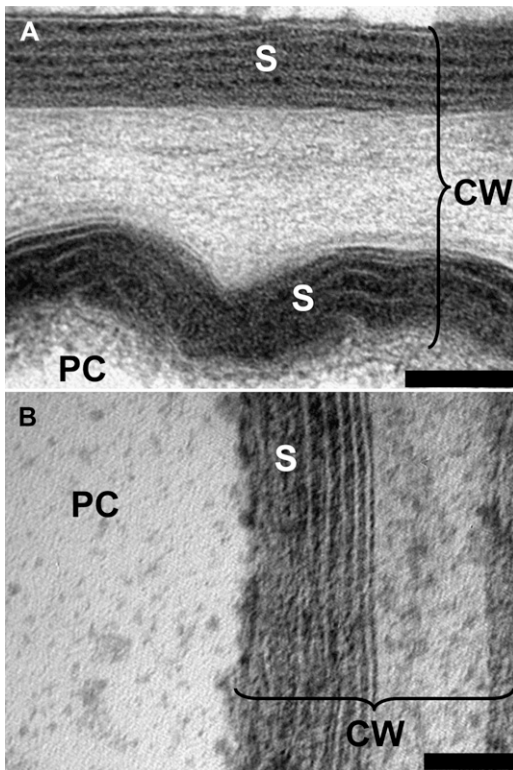
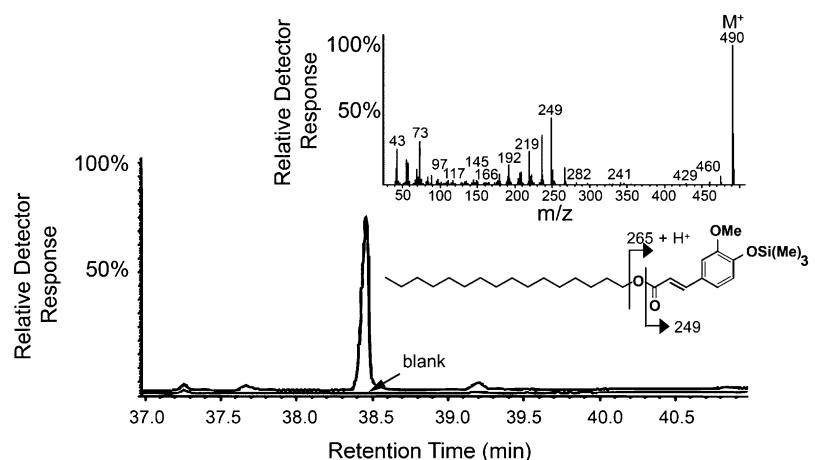


Figure 4. Transmission electron micrographs of *Arabidopsis* roots in the later stages of secondary thickening. The fine structure of suberin in the *asft-1* knockout mutant (B) is similar to the wild type (A). Samples were treated with hydrogen peroxide before the staining procedure (Heumann, 1990). Scale bar = 100 nm (A), 50 nm (B). CW, Cell wall; PC, peridermal cell; S, suberin.

methyl ester (Supplemental Fig. S5) as acyl acceptor. Higher conversions were noted for dodecan-1-ol, tetradecan-1-ol, and methyl 15-hydroxypentadecanoate, when compared to hexadecan-1-ol, whereas octadecan-1-ol showed only a trace of product. In all cases the substrate of the coupled assay was predominantly *trans*-ferulate and the product retained this stereochemistry. Thus we show that ASFT exhibits feruloyl-

Figure 5. Formation of hexadecyl ferulate ester by the recombinant ASFT enzyme in cell-free extracts. Recombinant ASFT protein was incubated with ferulate, ATP, CoASH, recombinant 4-coumarate ligase, and 1-hexadecanol. The GC-MS chromatogram of the extracted product shows a peak at 38.5 min that is absent if any of the above assay components are not present (blank). Insets: EI mass spectrum and molecular structure deduced from the fragmentation pattern of hexadecyl ferulate trimethylsilyl ether. Diagnostic ions: m/z 490, molecular ion; 266, [TMSi-ferulyloxy + H]⁺; 265, [TMSi-ferulyloxy]⁺; 249, [TMSi-feruloyl]⁺.



CoA-dependent feruloyl transferase activity toward substrates with a primary fatty alcohol functional group.

CYP86B1 Is Required for the Synthesis of Very-Long-Chain ω -Oxidized Suberin Monomers

Among cytochrome P450 monooxygenase CYP86 family members only expression of *CYP86A1* and *CYP86B1* is strongly correlated to the suberin bait set of genes (Supplemental Table S1). *CYP86A1* does not appear to be responsible for the high levels of very-long-chain α,ω -bifunctional suberin monomers in seeds (Li et al., 2007a; Höfer et al., 2008). Thus we investigated whether *CYP86B1* (*AT5G23190*) would provide this function. As 24-hydroxytetracosanoate is the major ω -OHFA of suberin in the outer integument of the seed coat (Molina et al., 2008) it might be a major site for ferulate esterification. A homozygous mutant allele was screened from the T-DNA insertion line SALK_130265 (*cyp86b1*; Supplemental Fig. S2C). The absence of *CYP86B1* transcripts in mRNA isolated from *cyp86b1* roots confirmed the selected line carried a null mutation of the gene (Supplemental Fig. S2D). No vegetative growth phenotype could be observed between the knockout mutant and wild type. Analysis of seeds for polyester monomers showed a very large reduction in α,ω -bifunctional C22 to C24 saturated suberin components (Fig. 6), with a corresponding increase in unsubstituted fatty acids. Reduction in very-long-chain monomers was also observed in polyester monomer analysis of mutant roots (Supplemental Fig. S6). To prove the changes in polyester monomers of the mutant are due to mutation of the gene *CYP86B1*, we also complemented the mutant plants with 35S::*CYP86B1* (Supplemental Fig. S6). Furthermore, proof of the function of this P450 was provided by an ectopic in planta expression experiment wherein *CYP86B1* was coexpressed with *GPAT5* under control of the 35S promoter. When cutin was analyzed, only the pairing of *GPAT5* and *CYP86B1* produced cutin monomer profiles containing very-

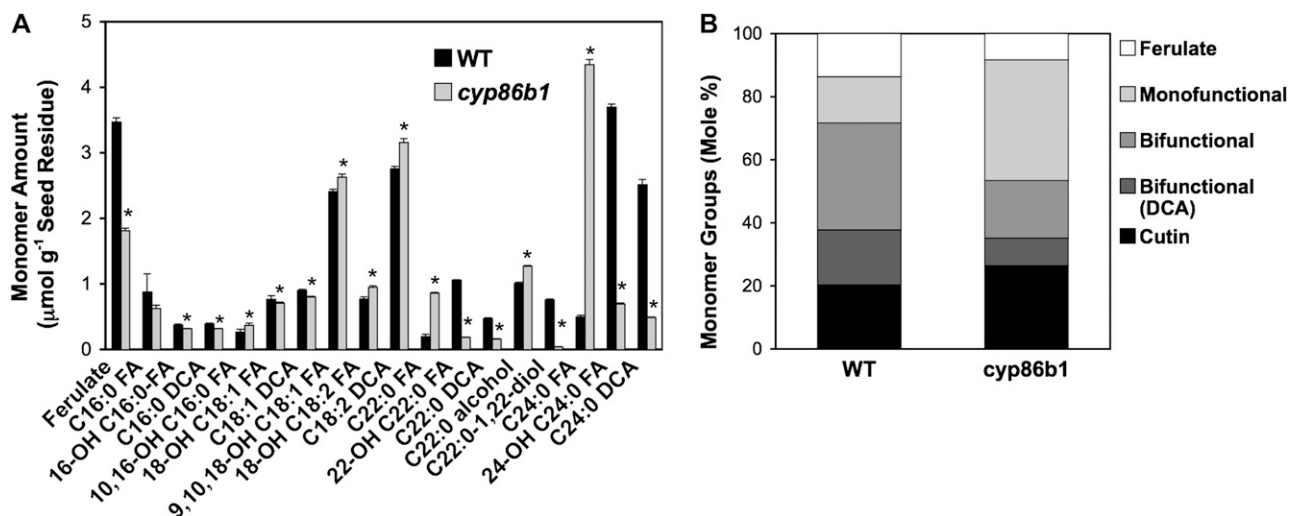


Figure 6. Comparison of lipid polyester monomer composition for wild-type and *cyp86b1* (*at5g23190*) seeds. *A*, Individual monomers. Means of triplicate determinations and SD are indicated. Asterisks denote a significant difference from wild type (WT; *t* test, two-sided, *P* < 0.05). *B*, Total monomer amounts, with monomers grouped into five classes. The cutin designation comprises 1,18-octadecadiene dioate and 9,10-,18-trihydroxyoctadecenoate, which are found in the cutin layers of the seed coat inner integument and the embryo, respectively. The other four classes comprise monomers from the suberized outer integument of the seed coat.

long-chain α,ω -bifunctional monomers (Fig. 7), confirming *in vivo* function.

DISCUSSION

ASFT Is a Feruloyl Transferase Involved in Suberin Biosynthesis

The BAHD gene *ASFT* was identified as playing a role in suberin biosynthesis based on chemical analy-

sis of mutants, on very specific cell-type expression patterns, and from *in vitro* activity of the recombinant enzyme. The promoter:*eYFP* expression experiments in *Arabidopsis* showed that the expression of this gene is localized to outer integument layer 1 of the seed coat and to the endodermis of young roots (Fig. 1), clearly defining it as a gene active only in suberin-synthesizing cells. Because mutation of *ASFT* reduces ferulate monomer associated with suberin by over 90% (Fig. 2) there is minimal functional redundancy with *AT5G63560*.

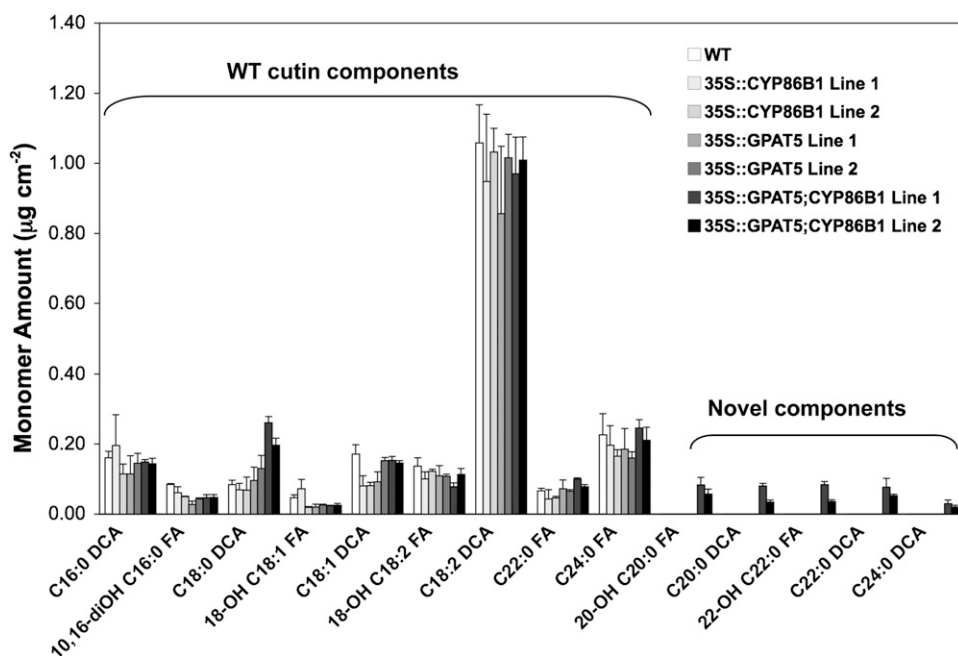


Figure 7. Changes in cutin content and composition in the stems of the single and coexpressors of GPAT5 and CYP86B1. Means of three experiments and SE are shown (8-week-old plants). WT, Wild type.

Thus, *ASFT* controls the major portion of ester-linked ferulate in suberin.

Several lines of evidence point to the *in vivo* function of ASFT as an *O*-acyltransferase required for the synthesis of aliphatic-aromatic ester linkages in suberin. We consider it unlikely that ASFT is directly involved in ferulate biosynthesis. Apart from its demonstrated activity as a feruloyl transferase to an aliphatic acyl acceptor, analysis of the genetic relationships in the BAHD gene family shows it is not closely related to the hydroxycinnamoyl transferase(s) that are implicated in monolignol biosynthesis (Supplemental Fig. S1; Hoffmann et al., 2003, 2004). Cell wall ferulate appears to share a common biosynthetic pathway with monolignols (Chen et al., 2006). Also, if ASFT was to function in ferulate biosynthesis we might expect a large reduction in 3'-hydroxylated phenylpropanoids. However, reductions in caffeate and ferulate and increases in coumarate are not seen in the root periderm waxes of *asft* mutants (Fig. 3). Tyramine is sometimes listed as an aromatic component of suberin, being found as amide with phenylpropanoid acids (Kolattukudy, 2001; Bernards, 2002). However, genes for hydroxycinnamoyl-CoA:tyramine *N*-hydroxycinnamoyl transferases have been cloned and the proteins are members of the diamine acetyltransferase family (Farmer et al., 1999; Schmidt et al., 1999), so there is no need to postulate ASFT as an *N*-acyltransferase. Our Arabidopsis seed polyester monomer analyses were set up to recover tyramine, but none was observed (Molina et al., 2006). Furthermore, based on the kinetics of product release during NaOMe-catalyzed transmethylation we inferred that most of the ferulate monomer released from Arabidopsis seed coats is from ester and not amide linkages (Molina et al., 2006).

Feruloyl transferase activity utilizing feruloyl-CoA as the acyl donor and ω -OHFA as acyl acceptor has been shown in extracts from potato tubers (Lotfy et al., 1994) and tobacco cell suspensions (Lotfy et al., 1996). During purification the tobacco activity behaved as a soluble enzyme, with an apparent molecular mass of 55 kD by size exclusion chromatography and a pI of 4.6. However, the proteins or their corresponding genes responsible for the hydroxycinnamoyl-transferase reaction have remained unidentified. Our enzymology results prove that ASFT can function as an *O*-acyltransferase that produces ω -feruloyloxy aliphatics. The fact that there is an approximately mole-for-mole reduction in ferulate and aliphatic molecules containing a primary alcohol functional group in the knockout mutants lends credence to the proposal that this activity observed *in vitro* is also operating *in vivo*. The fact that the deduced Arabidopsis ASFTp has an estimated molecular mass of 51 kD and pI of 5.5 is very consistent with the data obtained for the tobacco enzyme.

So far we have been unable to scale down the partial depolymerization methods that work on large suberin samples (such as cork) to Arabidopsis seeds. Such

methods have allowed a tentative accounting of oligomers. Feruloyl groups appear to be esterified to ω -hydroxy groups of aliphatic monomers with an order of magnitude greater frequency than to the hydroxyl groups of glycerol (Graça and Pereira, 1999, 2000). Even as we postulate that the *in vivo* function of ASFT is the synthesis of ω -feruloyloxy aliphatics, and show that it can synthesize alkyl ferulate *in vitro* (Fig. 5) and that it is expressed in root periderm cells (Fig. 1), the knockout mutant of *ASFT* has no effect on the deposition of the alkyl coumarates, caffeates, and ferulates of the suberin-associated waxes of the root periderm (Li et al., 2007b). Thus we hypothesize that another BAHD enzyme, and possibly AT5G63560, might have a different specificity and might be largely responsible for suberin wax formation in the root periderm.

In examining the monomer profile of *asft* (Fig. 2), it should be noted that in wild-type seeds ferulate deposition probably does not fully overlap with aliphatic monomer deposition. This is the case in *Brassica napus* (Molina et al., 2008), where the onset of ferulate and aliphatic deposition are identical but where fatty alcohol and ω -OHFA accumulation continues well after ferulate and DCA deposition has stopped. In allele *asft-1* (Fig. 2) the increase in very-long-chain DCA monomer levels as ω -OHFAs are reduced implies an indirect compensatory effect, suggesting that feruloyl transfer and further ω -oxidation to DCA compete for the same pool of ω -OHFA. An interesting parallel exists with an experiment using inhibitors of phenylpropanoid biosynthesis in green cotton fibers (Schmutz et al., 1996), where a reduction of hydroxycinnamic acids in suberin was accompanied by a decrease in ω -OHFAs and an increase in DCAs. Furthermore, the approximately equimolar loss of ferulate and an aliphatic group in the *asft* knockout mutants implies that a feruloyloxy aliphatic is a biosynthetic unit required for suberin assembly and that feruloylation accelerates flux through that branch of the aliphatic pathway.

CYP86B1 (AT5G23190) Is Required for Very-Long-Chain α,ω -Bifunctional Monomer Synthesis in Seed Suberin

Our results and those of a very recent study (Compagnon et al., 2009) identify *CYP86B1* (AT5G23190) as a gene required for suberin very-long-chain α,ω -bifunctional monomer synthesis. The ectopic coexpression experiment with GPAT5 and CYP86A1 shows that CYP86A1 produces C16 to C22 monomers in cutin (Li et al., 2007a), while the same experiment with GPAT5 and CYP86B1 shows that CYP86B1 produces C18 to C24 monomers (Fig. 7). However, in seeds it is CYP86B1 that is required for the biosynthesis of most of the C22:0 and C24:0 ω -OHFAs and DCAs (Fig. 6). The knockout of this gene results in the accumulation of the corresponding C22:0 and C24:0 fatty acids, which may or may not be the immediate acyl precursor for the ω -hydroxylase. As we have previously noted, defining the exact biochemical

pathway on the basis of changes in monomer distribution of mutants is extraordinarily difficult (Pollard et al., 2008). CYP86B1 surely functions as an ω -hydroxylase and requires GPAT5 for function, but whether it also functions as an ω -oxidase to produce DCAs, and whether the hydroxylation precedes or succeeds either GPAT5-catalyzed acyl transfer or the fatty acid elongase(s) remains to be determined.

The reduction in ferulate when C22:0 and C24:0 ω -OHFAs are reduced by *cyp86b1*, and the reduction in C22:0 and C24:0 ω -OHFAs when ferulate is reduced by *asft*, suggest that a significant portion of ferulate in wild type is esterified to C22:0 and C24:0 ω -OHFAs. In our studies of *Arabidopsis* and *B. napus* seed polyesters we were able to localize the monomers to three distinct locations in the seed (Molina et al., 2008). These studies were based on seed dissections, a mutant impaired in the formation of the outer integument of the seed coat, and promoter:GFP-based localization of gene expression. 9,10,18-Trihydroxyoctadecenoate and C18:2 DCA, which are cutin monomers, were dominantly associated with the inner layer of the seed coat inner integument and the embryo, respectively. The remaining monomers were those typical of suberin and were localized to the inner layer of the outer integument. Using this information we can subtract the contributions of the two major cutin monomers from the total seed monomer profile to give an approximate composition of suberin monomers of the seed coat outer integument. Thus we classify the monomers detailed in Figure 6A as shown in Figure 6B. There is little precedence in the natural products literature for hydroxycinnamic acids to be esterified through their phenolic hydroxyl groups. This is hardly surprising, since their main biological function is predicated through free radical formation from the free phenolic hydroxyl group, to allow oxidative coupling reactions. Thus we count ferulate as monofunctional in this suberin monomer classification. Ferulate, which accounts for about 13.7 mol % of monomers in total polyesters of wild-type seed, becomes 16.5 mol % of just the suberin monomers. If we classify monofunctional monomers as normal fatty acids and fatty alcohols, and subtract out the cutin component, then the monofunctional monomers in seed suberin account of 35.6 mol % in wild type, but rise to 63.2 mol % in *cyp86b1*, mainly through the accumulation of tetracosanoic acid.

Implications for Models of Suberin Structure

A model describing the lamellar suberin structure for potato periderm has a ferulate-monolignol polyphenolic domain embedded in the primary cell wall and covalently linked to a glycerol-based polyaliphatic domain (Bernards, 2002). The aliphatic polyesters extend across multiple electron-translucent bands. The opaque bands may correspond to glycerol, esterified phenolics, and waxes. A model for cork suberin (Graça and Santos, 2007) presents a single aliphatic-chain-

wide translucent domain where the polyacylglycerol mainly folds back on itself, and a wider, variable-width electron-rich domain that contains the cross-linked hydroxycinnamic acids. In both models ferulic acid has been suggested to provide crucial covalent links between polyaromatics and the suberin aliphatic polyester. These links are esterification through the ferulate carboxylate group and one electron oxidation of the phenolic group to allow radical coupling of the ferulate to produce nonester bonded dimers and oligomers. In both models there is an implication of overlapping aliphatic and aromatic precursor biosynthesis. In view of our observation that, at least in root tissue, the suberin lamellae appear largely unaffected by the *at5g41040* mutant, the importance of ester-linked ferulate in the formation of the lamellae must be reconsidered. Whether the reduction in ferulate released by transesterification does or does not affect the lamellar structure of suberin in tissues other than roots remains to be determined. Histochemical analyses (Lulai and Corsini, 1998) and principal component analysis of precursors (Yang and Bernards, 2007) during potato wound suberization support the view that deposition of the aromatic domain is the first event in suberization. Indeed, Lulai and Freeman (2001) have proposed that there is no covalent connectivity between the polyaromatic and polyaliphatic domains. Our observation that ferulate deposition ceases as aliphatics are still being laid down in *Brassica* seeds (Molina et al., 2008) is consistent with polyaromatic deposition preceding polyaliphatic deposition.

An important observation is that the suberin aliphatic monomer amount has not been greatly reduced in *asft* mutants. A corollary is that the loss of ferulate does not impact the insolubility of the suberin polyester. The fact that suberin aliphatic deposition in late-stage *Brassica* seeds does not overlap ferulate deposition is consistent with this deduction (Molina et al., 2008). This raises questions concerning the role of ferulic acid in attaching aliphatics to the cell wall. Even if most of the ferulate is incorporated into suberin as ω -feruloyloxy aliphatics, a very small amount of cross linking might cause suberin insolubility. Ferulate derivatives that have been oxidatively cross linked (Bernards et al., 1995) will either not be released from the polymer matrix by transmethylation, or if they are released, they will not be detected by our GC-MS analysis. Thus it remains possible that ASFT or another enzyme may attach ferulate to other sites in suberin currently unknown but possibly glycerol, and where oxidation to form cross links is prevalent. Further studies are required to assess the breadth of acyl acceptor specificity of ASFT, both for potential ω -OHFA substrates such as free acids, acylglycerols, and acyl-CoAs, and to test whether acceptors other than aliphatics with a primary OH group might also be substrates. However, it is clear that ASFT and AT5G63560 have nonredundant functions, at least in regards to the presence of ferulate released by transmethylation. Thus it is possible AT5G63560 might

function to provide ferulate for cross linking, or to provide sufficient redundancy with ASFT in *asft* knockout lines, to keep the suberin insoluble.

Even as our results for ASFT require that we reconsider the role of ferulate in suberin structure and its properties, our results with CYP86B1 are inconsistent with the concept of an extended polyaliphatic domain, at least for Arabidopsis seed suberin. In a condensation polymer monofunctional monomers terminate a polymer chain. An ω -OHFA cannot cause cross linking, but a combination of glycerol and α,ω -DCAs may result in cross linking (Pollard et al., 2008). If we allow a condensation polymer to form between just the observed monomers and glycerol, wild-type suberin clearly has the potential to form an extended polyaliphatic domain. However, in *cyp86b1*, where the suberin is still an insoluble product, the large mole fraction of monofunctional monomers ($\geq 60\%$) should preclude polymer formation, let alone cross-linked polymer formation. Thus either an additional contribution from a hidden aliphatic component (suberan) or an additional matrix is required to describe suberin. Furthermore, if we suggest that wild-type suberin really does not exist as an extended polyaliphatic, the idea that a very-low density of cross-linked ferulates could anchor the material, causing its insolubility, also seems less likely. Clearly, suberin structure needs a reinvestigation.

MATERIALS AND METHODS

Plant Materials and Growth Conditions

Arabidopsis (*Arabidopsis thaliana*) wild-type (Columbia-0) and mutant seeds were germinated and grown as described by Li et al. (2007a). Transgenic seeds were stratified and germinated on Murashige and Skoog (MS) medium supplemented with either with 50 $\mu\text{g mL}^{-1}$ kanamycin or 30 $\mu\text{g mL}^{-1}$ hygromycin or a combination of both in the case of double overexpressors. Selected plants were transferred to soil and grown as indicated above.

Mutant Isolation

Seed stocks of three T-DNA insertion lines (Alonso-Blanco et al., 2003) for *ASFT* (AT5G41040; SALK_048898 and SALK_017725) and for *CYP86B1* (AT5G23190; SALK_130265) were obtained from the Arabidopsis Biological Resource Center seed collection (<http://www.biosci.ohiostate.edu>). Primers to amplify the wild-type gene were ASFT-F1 and ASFT-R1, and CYP86B1-scF and CYP86B1-scR, respectively (Supplemental Table S2). To check for the insertion, the primer set used was ASFT-R2, specific for the 3'-untranslated region gene sequence, or CYP86B1-scR and the T-DNA left-border-specific primer LBa1. For the RT-PCR, RNA was isolated from 100 mg of 3-week-old Arabidopsis roots using the RNeasy plant mini kit (Qiagen), following manufacturer's instructions. SuperScript III reverse transcriptase (Invitrogen) was used to synthesize the first-strand cDNA, following manufacturer's protocol. Two-microliter aliquots of the RT reactions were used as template for PCR. Primers for *ASFT* amplification were ASFT-F3 and ASFT-R3, for CYP86B1, CYP86B1-F and CYP86B1-R (Supplemental Table S2). The house-keeping eukaryotic eIF4A gene was used as a control.

eYFP Reporter Construct Design and Plant Transformation

The reporter gene *eYFP* was amplified by PCR and cloned into *Bam*HI-*Sac*I-digested pBI101. The primers used for the amplification were YFP-F (forward)

and YFP-R (reverse; Supplemental Table S2). The 2.0-kb 5' sequence of the *ASFT* DNA was amplified by PCR using genomic DNA as template (*PRO_{ASFT}*) and subcloned in pGEM-T easy vector (Promega Corporation) for sequencing. Cloning primers were ASFT-F (forward) and ASFT-R (reverse; Supplemental Table S2). All amplifications used a proofreading DNA polymerase (Platinum Pfx). To generate the *PRO_{ASFT}::eYFP* construct, the promoter sequences were released from pGEM-T easy vectors and ligated into *Sall*-*Bam*HI-digested pBI101-*eYFP*, upstream of the *eYFP* sequence. The binary plasmid was introduced into *Agrobacterium tumefaciens* strain C58C1 by electroporation. Arabidopsis Columbia-0 wild-type transformation was performed by the vacuum-infiltration method (Bechtold et al., 1993). T2 seeds from several individual kanamycin-resistant plants were analyzed by CLSM to evaluate YFP expression.

Confocal Microscopy Analysis of eYFP Reporter Expression

Imaging of whole-developing transgenic seeds and roots mounted in water was performed with Zeiss Pascal confocal laser-scanning microscope (Carl Zeiss International), using a 20 \times Plan-Neofluar Carl Zeiss objective. Samples were excited with 488-nm argon ion laser line and emission was detected after passing through a BP 505 to 530 (digitally colored green), and long-pass 650-nm filter (digitally colored red). Individual optical sections were used to create extended focus images using LSM 5 Pascal (version 3.0) software. Images were overlaid to derive a two-color image. All samples were treated with 0.5 mg mL⁻¹ aqueous propidium iodide (Sigma) for 10 min to visualize cell walls. Images were transformed to TIFF format files and processed with Adobe Photoshop CS2.

TEM

Root samples (1 mm² size) were fixed with 0.1 M cacodylate buffer containing 2.5% glutaraldehyde and 2% paraformaldehyde, post fixed with 1% buffered osmium tetroxide, and dehydrated through a graded acetone series. Samples were then infiltrated with Poly/Bed 812 resin. After placing in silicone moulds, embedded samples were polymerized for 24 h at 60°C. Silver-gold ultrathin sections were prepared with a diamond knife on a Power Tome_XL microtome (Boeckeler Instruments) and placed on copper-mesh grids. Samples on grids were treated with 10% hydrogen peroxide for 10 min, and stained with 10% uranyl acetate in methanol for 8 min, and Reynold's lead citrate for 10 min. This modified staining procedure enables to enhance the contrast of both cutin and suberin (Heumann, 1990). Specimens were examined with a JEOL 100CX transmission electron microscope, and images processed with Adobe Photoshop CS2.

Lipid Analysis

Sodium methoxide catalyzed depolymerization and GC-MS or GC-flame ionization detector analyses were performed on whole-delipidated seed, stem, or root tissues following the protocol detailed in Molina et al. (2006). The major ferulate isomer is always the trans-isomer (≥ 92 mol %). The contribution of the minor cis-ferulate isomer is not included in composition tabulations. Root wax extraction and analyses were performed according to Li et al. (2007b). The alkyl hydroxycinnamate esters are predominantly the trans-isomers. These stereochemical assignments are based on the observation that the alkyl esters of cis-ferulate always elute ahead of the trans-isomers on nonpolar GC columns.

Recombinant Protein Expression

The *ASFT* cDNA designed de novo to optimize the codon usage for *Escherichia coli* was synthesized by GenScript. The synthetic *ASFT* cDNA was cloned into pGS-21a expression vector (GenScript) using *Nco*I and *Xho*I restriction sites. A His tag/glutathione S-transferase epitope was fused in frame at the N terminus. *E. coli* BL21 (DE3) LysS (Novagen) cells were transformed by heat shock with 0.2 μg of plasmid and grown in Luria-Bertani plates containing 100 $\mu\text{g mL}^{-1}$ carbenicillin and 34 $\mu\text{g mL}^{-1}$ chloramphenicol. A single bacterial colony was used to inoculate a liquid culture, which was in turn used to inoculate a subculture of Luria-Bertani medium containing 100 $\mu\text{g mL}^{-1}$ carbenicillin, which was grown at 20°C with shaking. When OD = 0.6, isopropyl β -D-thiogalactopyranoside (0.8 mM) was added for induction of

protein expression, and culture was grown for 24 h. Procedures for protein extraction and subsequent purification are described elsewhere (Beuerle and Pichersky, 2002). The soluble recombinant protein was purified by Ni²⁺ chelating chromatography, and the presence of the fusion protein was confirmed by SDS-PAGE and western blot.

Feruloyl Transferase Assay

Feruloyl-CoA substrate was generated by incubating a reaction mixture (1 mL) containing 50 mM Tris-HCl pH 7.5, 2.5 mM MgCl₂, 2.5 mM ATP, 0.2 mM ferulic acid, 0.2 mM CoA, and 10 μL of purified recombinant 4-coumarate ligase (Beuerle and Pichersky, 2002) for 1 h at 30°C. To initiate ester synthesis, 10 μL of recombinant ASFT-tagged protein, 1 mM dithiothreitol, and 1 mM fatty alcohol or methyl 15-hydroxypentadecanoate were added. After incubation overnight at 30°C the reaction was stopped by addition of 2 mL chloroform:methanol (2:1, v/v). The organic phase was removed and dried under N₂ stream. Samples were silylated by heating at 110°C for 10 min with *N,O*-bis(trimethylsilyl)trifluoroacetamide:pyridine (1:1, v/v) and analyzed by GC-MS(EI) on a HP-5MS capillary column temperature programmed from 130°C to 330°C at 5°C/min.

CYP86B1 Overexpression Construct Design, Complementation, and Plant Transformation

Genomic DNA was prepared from Arabidopsis leaf tissue using a plant mini DNA kit according to the manufacturer's instructions (Qiagen). Genomic DNA sequences encoding the *CYP86B1* gene (AT5G23190) were amplified by PCR using primers CYP86B1-cF and CYP86B1-cR (Supplemental Table S2). The PCR product was cloned as a *Bgl*II-*Spe*I fragment into binary vector pCambia1302 (Cambia). The construct was named as 35S::CYP86B1. This construct and also the 35S::GPAT5 construct (Li et al., 2007b) were individually introduced into *A. tumefaciens* strain C58C1 for Arabidopsis vacuum infiltration (Bechtold et al., 1993). Wild-type Arabidopsis plants were dipped into MS suc solution containing transgenic agrobacteria harboring 35S::CYP86B1; plants were also dipped into cultures containing equal amounts of 35S::CYP86B1/35S::GPAT5. Transgenic plants were then selected on MS agar plates containing 30 μg mL⁻¹ hygromycin alone for CYP86B1 transformants, or selected on MS plates containing both 30 μg mL⁻¹ hygromycin and 50 μg mL⁻¹ kanamycin for double transformants. For complementation, *cyp86b1* mutant plants were infiltrated with agrobacterium harboring 35S::CYP86B1.

Supplemental Data

The following materials are available in the online version of this article.

Supplemental Figure S1. Phylogenetic analysis of the Arabidopsis BAHD family.

Supplemental Figure S2. Structure of the *ASFT* and *CYP86B1* T-DNA insertion mutants, and analysis of gene expression by RT-PCR.

Supplemental Figure S3. Root suberin monomer composition of wild-type and *asf1* knockout mutants.

Supplemental Figure S4. TEM of suberized peridermal cells in 7-week-old roots of wild-type and *cyp86a1* plants.

Supplemental Figure S5. In vitro formation of 15-feruloyloxypentadecanoic acid methyl ester by the recombinant ASFT enzyme.

Supplemental Figure S6. Root suberin monomer composition of wild type, *cyp86b1* knockout, and the complemented lines 35S::CYP86B1.

Supplemental Table S1. Correlation of gene expression using suberin-associated genes as bait: some representative results.

Supplemental Table S2. Primer sequences.

ACKNOWLEDGMENTS

We thank Alicia Pastor (Michigan State University Advanced Microscopy Center) for her assistance in sectioning samples for TEM and Dr. Eran Pichersky (University of Michigan) for providing us with an *E. coli* strain expressing a tobacco 4-coumarate ligase.

Received July 16, 2009; accepted September 13, 2009; published September 16, 2009.

LITERATURE CITED

- Alonso-Blanco C, Bentsink L, Hanhart CJ, Blankestijn-de Vries H, Koornneef M (2003) Analysis of natural allelic variation at seed dormancy loci of *Arabidopsis thaliana*. *Genetics* **164**: 711–729
- Bechtold N, Ellis J, Pelletier G (1993) *In planta* Agrobacterium-mediated gene transfer by infiltration of adult *Arabidopsis thaliana* plants. *C R Acad Sci Ser III* **316**: 1194–1199
- Beisson F, Li YH, Bonaventure G, Pollard M, Ohlrogge JB (2007) The acyltransferase GPAT5 is required for the synthesis of suberin in seed coat and root of *Arabidopsis*. *Plant Cell* **19**: 351–368
- Bernards M (2002) Demystifying suberin. *Can J Bot* **80**: 227–240
- Bernards MA, Lopez ML, Zajicek J, Lewis NG (1995) Hydroxycinnamic acid-derived polymers constitute the polyaromatic domain of suberin. *J Biol Chem* **270**: 7382–7386
- Beuerle T, Pichersky E (2002) Enzymatic synthesis and purification of aromatic coenzyme A esters. *Anal Biochem* **302**: 305–312
- Chen F, Srinivasa Reddy M, Temple S, Jackson L, Shadle G, Dixon R (2006) Multi-site genetic modulation of monolignol biosynthesis suggests new routes for formation of syringyl lignin and wall-bound ferulic acid in alfalfa (*Medicago sativa* L.). *Plant J* **48**: 113–124
- Compagnon V, Diehl P, Benveniste I, Meyer D, Schaller H, Schreiber L, Franke R, Pinot F (2009) CYP86B1 is required for very long chain ω-hydroxyacids and α,ω-dicarboxylic acids synthesis in root and seed suberin polyester. *Plant Physiol* **150**: 1831–1843
- D'Auria JC (2006) Acyltransferases in plants: a good time to be BAHD. *Curr Opin Plant Biol* **9**: 331–340
- Espelie KE, Davis RW, Kolattukudy PE (1980) Composition, ultrastructure and function of the cutin- and suberin-containing layers in the leaf, fruit peel, juice-sac and inner seed coat of the grapefruit (*Citrus paradisi* Macf.). *Planta* **149**: 498–511
- Farmer MJ, Czernic P, Michael A, Negrel J (1999) Identification and characterization of cDNA clones encoding hydroxycinnamoyl-CoA: tyramine N-hydroxycinnamoyltransferase from tobacco. *Eur J Biochem* **263**: 686–694
- Franke R, Briesen I, Wojciechowski T, Faust A, Yephremov A, Nawrath C, Schreiber L (2005) Apoplastic polyesters in Arabidopsis surface tissues—a typical suberin and a particular cutin. *Phytochemistry* **66**: 2643–2658
- Franke R, Schreiber L (2007) Suberin—a biopolyester forming apoplastic plant interfaces. *Curr Opin Plant Biol* **10**: 252–259
- Graça J, Pereira H (1999) Glycerol-acyl and aryl-acyl dimers in *Pseudotsuga menziesii* bark suberin. *Holzforschung* **53**: 397–402
- Graça J, Pereira H (2000) Suberin structure in potato periderm: glycerol, long-chain monomers, and glyceryl and feruloyl dimers. *J Agric Food Chem* **48**: 5476–5483
- Graça J, Santos S (2006) Glycerol-derived ester oligomers from cork suberin. *Chem Phys Lipids* **144**: 96–107
- Graça J, Santos S (2007) Suberin: a biopolyester of plants' skin. *Macromol Biosci* **7**: 128–135
- Graça J, Schreiber L, Rodrigues J, Pereira H (2002) Glycerol and glyceryl esters of omega-hydroxyacids in cutins. *Phytochemistry* **61**: 205–215
- Heumann HG (1990) A simple method for improved visualization of the lamellated structure of cutinized and suberized plant-cell walls by electron-microscopy. *Stain Technol* **65**: 183–187
- Höfer R, Briesen I, Beck M, Pinot F, Schreiber L, Franke R (2008) The Arabidopsis cytochrome P450 CYP86A1 encodes a fatty acid omega-hydroxylase involved in suberin monomer biosynthesis. *J Exp Bot* **59**: 2347–2360
- Hoffmann L, Besseau S, Geoffroy P, Ritzenthaler C, Meyer D, Lapierre C, Pollet B, Legrand M (2004) Silencing of hydroxycinnamoyl-coenzyme A shikimate/quinic hydroxycinnamoyltransferase affects phenylpropanoid biosynthesis. *Plant Cell* **16**: 1446–1465
- Hoffmann L, Maury S, Martz F, Geoffroy P, Legrand M (2003) Purification, cloning, and properties of an acyltransferase controlling shikimate and quinate ester intermediates in phenylpropanoid metabolism. *J Biol Chem* **278**: 95–103
- Kolattukudy PE (1981) Structure, biosynthesis, and biodegradation of cutin and suberin. *Annu Rev Plant Physiol Plant Mol Biol* **32**: 539–567

- Kolattukudy PE** (2001) Polyesters in higher plants. *Adv Biochem Eng Biotechnol* **71**: 1–49
- Li Y, Beisson F, Koo AJ, Molina I, Pollard M, Ohlrogge J** (2007a) Identification of acyltransferases required for cutin biosynthesis and production of cutin with suberin-like monomers. *Proc Natl Acad Sci USA* **104**: 18339–18344
- Li Y, Beisson F, Ohlrogge J, Pollard M** (2007b) Monoacylglycerols are components of root waxes and can be produced in the aerial cuticle by ectopic expression of a suberin-associated acyltransferase. *Plant Physiol* **144**: 1267–1277
- Lofy S, Javelle F, Negrel J** (1996) Purification and characterization of hydroxycinnamoyl-coenzyme A: ω -hydroxypalmitic acid O-hydroxycinnamoyltransferase from tobacco (*Nicotiana tabacum* L.) cell-suspension cultures. *Planta* **199**: 475–480
- Lofy S, Negrel J, Javelle F** (1994) Formation of omega-feruloyloxypalmitic acid by an enzyme from wound-healing potato-tuber disks. *Phytochemistry* **35**: 1419–1424
- Lulai EC, Corsini DL** (1998) Differential deposition of suberin phenolic and aliphatic domains and their roles in resistance to infection during potato tuber (*Solanum tuberosum* L.) wound-healing. *Physiol Mol Plant Pathol* **53**: 209–222
- Lulai EC, Freeman TP** (2001) The importance of phellogen cells and their structural characteristics in susceptibility and resistance to excoriation in immature and mature potato tuber (*Solanum tuberosum* L.) periderm. *Ann Bot (Lond)* **88**: 555–561
- Ma F, Peterson C** (2003) Current insights into the development, structure, and chemistry of the endodermis and exodermis of roots. *Can J Bot* **81**: 405–421
- Matzke K, Riederer M** (1991) A comparative-study into the chemical constitution of cutins and suberins from *Picea abies* (L.) Karst, *Quercus robur* L, and *Fagus sylvatica* L. *Planta* **185**: 233–245
- Molina I, Bonaventure G, Ohlrogge J, Pollard M** (2006) The lipid polyester composition of *Arabidopsis thaliana* and *Brassica napus* seeds. *Phytochemistry* **67**: 2597–2610
- Molina I, Ohlrogge JB, Pollard M** (2008) Deposition and localization of lipid polyester in developing seeds of *Brassica napus* and *Arabidopsis thaliana*. *Plant J* **53**: 437–449
- Nawrath C** (2002) The biopolymers cutin and suberin. In CR Somerville, EM Meyerowitz, eds, *The Arabidopsis Book*. American Society of Plant Biologists, Rockville, MD, doi: 10.1199/tab.0021, <http://www.aspb.org/publications/arabidopsis/>
- Pollard M, Beisson F, Li Y, Ohlrogge JB** (2008) Building lipid barriers: biosynthesis of cutin and suberin. *Trends Plant Sci* **13**: 236–246
- Schmid M, Davison TS, Henz SR, Pape UJ, Demar M, Vingron M, Schölkopf B, Weigel D, Lohmann J** (2005) A gene expression map of *Arabidopsis* development. *Nat Genet* **37**: 501–506
- Schmidt A, Grimm R, Schmidt J, Scheel D, Strack D, Rosahl S** (1999) Cloning and expression of a potato cDNA encoding hydroxycinnamoyl-CoA:tyramine N-(hydroxycinnamoyl)transferase. *J Biol Chem* **274**: 4273–4280
- Schmutz A, Buchala AJ, Ryser U** (1996) Changing the dimensions of suberin lamellae of green cotton fibers with a specific inhibitor of the endoplasmic reticulum-associated fatty acid elongases. *Plant Physiol* **110**: 403–411
- Schmutz A, Titus J, Ryser U** (1994) A caffeoyl-fatty acid-glycerol ester from wax associated with green cotton fibre suberin. *Phytochemistry* **36**: 1341–1346
- Schreiber L, Franke R, Hartmann K** (2005) Effects of NO₃ deficiency and NaCl stress on suberin deposition in rhizo- and hypodermal (RHCW) and endodermal cell walls (ECW) of castor bean (*Ricinus communis* L.) roots. *Plant Soil* **269**: 333–339
- Serra O, Soler M, Hohn C, Sauveplane V, Pinot F, Franke R, Schreiber L, Prat S, Molinas M, Figueras M** (2009) CYP86A33-targeted gene silencing in potato tuber alters suberin composition, distorts suberin lamellae, and impairs the periderm's water barrier function. *Plant Physiol* **149**: 1050–1060
- Soler M, Serra O, Molinas M, Huguet G, Fluch S, Figueras M** (2007) A genomic approach to suberin biosynthesis and cork differentiation. *Plant Physiol* **144**: 419–431
- St Pierre B, De Luca V** (2000) Evolution of acyltransferase genes: origin and diversification of the BAHF superfamily of acyltransferases involved in secondary metabolism. In JT Romeo, L Varin, V De Luca, eds, *Recent Advances in Phytochemistry, Vol 34. Evolution of Metabolic Pathways*. Elsevier Science Ltd., pp 285–315
- Wei H, Persson S, Mehta T, Srinivasasainagendra V, Chen L, Page GP, Somerville C, Loraine A** (2006) Transcriptional coordination of the metabolic network in *Arabidopsis*. *Plant Physiol* **142**: 762–774
- Yang WL, Bernards MA** (2007) Metabolite profiling of potato (*Solanum tuberosum* L.) tubers during wound-induced suberization. *Metabolomics* **3**: 147–159
- Yu XH, Gou JY, Liu CJ** (2009) BAHF superfamily of acyl-CoA dependent acyltransferases in *Populus* and *Arabidopsis*: bioinformatics and gene expression. *Plant Mol Biol* **70**: 421–442

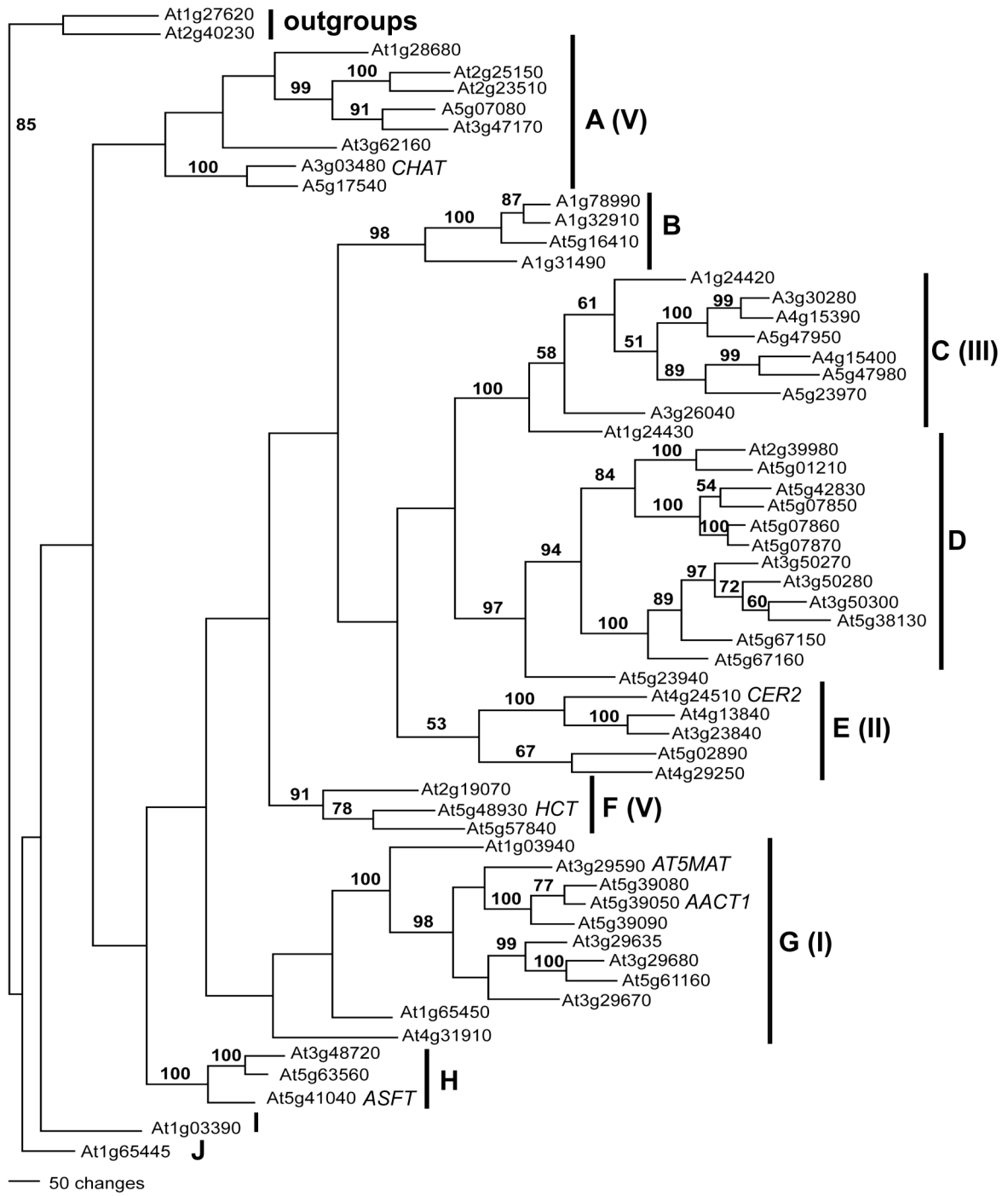


Figure S1: Phylogenetic analysis of the Arabidopsis BAHD family. Deduced protein sequences of the Arabidopsis BAHD family were retrieved in FASTA format from the GenBank database and a multiple alignment was created by ClustalX (Thompson et al., 1997) using the default settings. The figure shows the majority-rule consensus tree of 10,772 best score trees, generated according to the maximum parsimony principle with PAUP Version 4.0b10 (Swofford, 2000), and using two proteins (encoded by At1g27620 and At2g40230 loci) as outgroups. A heuristic bootstrap search was performed with 1000 replicates, 100 random addition replicates per bootstrap replicate. Numbers on branches indicate bootstrap values as percentages (bootstrap values lower than 50% are not shown). Numbers between parentheses correspond to the clades (I-V) described by D'Auria (D'Auria, 2006). AACT1: Anthocyanin 5-aromatic acyltransferase1; AT5MAT: O-malonyltransferase; CHAT: Acetyl-CoA:(Z)-3-hexen-1-ol acetyltransferase; HCT: hydroxycinnamoyl-CoA:shikimate/quinic acid hydroxycinnamoyltransferase; *Cer2*: *Eciferum2*.

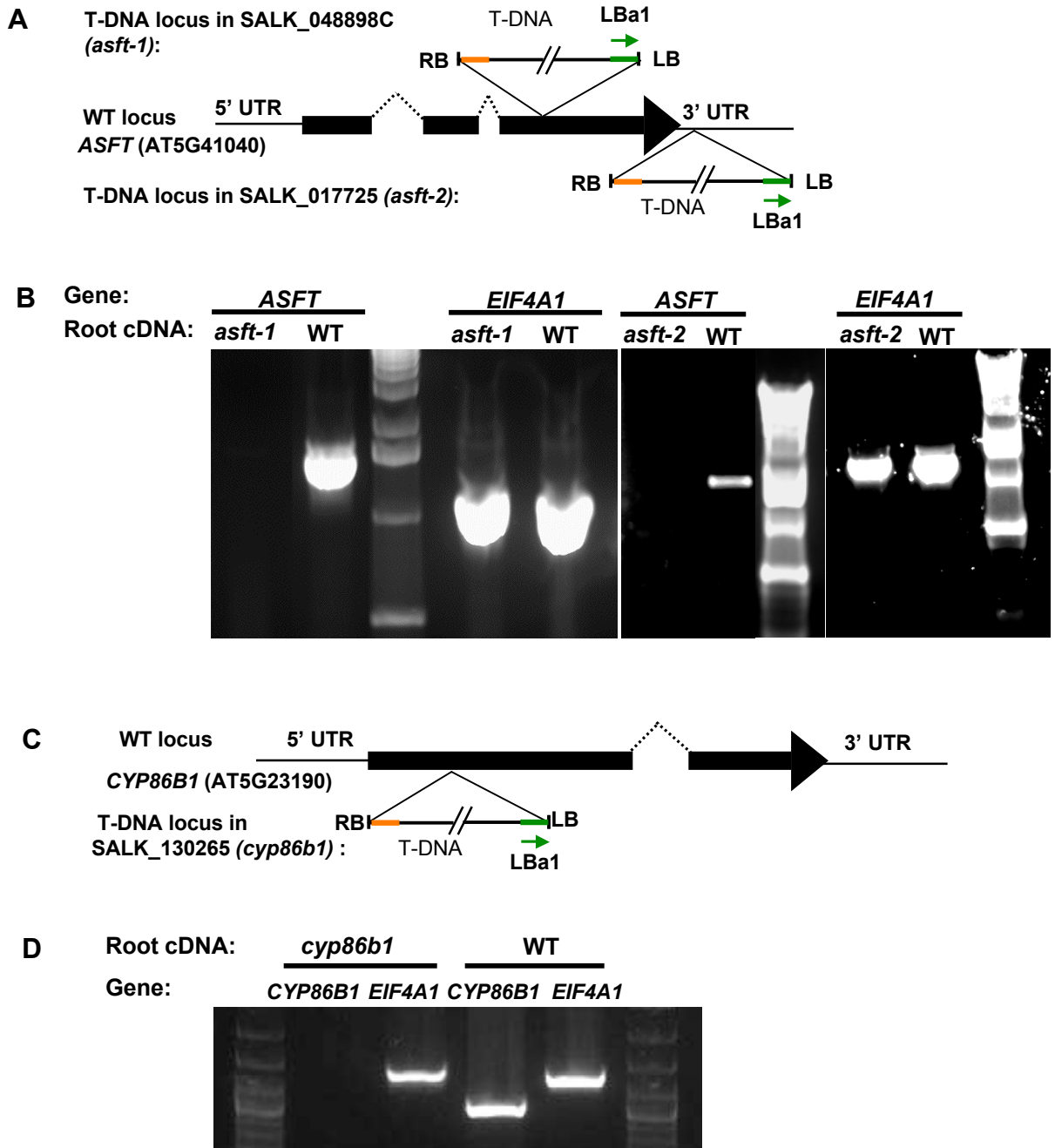


Figure S2: Structure of *ASFT* and *CYP86B1* genes showing the site of T-DNA insertion and analysis of gene expression by RT-PCR. (A) Genomic organization of the *ASFT* gene (At5g41040 locus) in the *asft* SALK lines. Homozygous plants for the T-DNA insertion in *ASFT* were obtained from the homozygous collection of ABRC (SALK_048898C) or were isolated from SALK_101725 heterozygous seeds. T-DNA insertions are in the third exon (*asft-1*) or 3' UTR (*asft-2*). **(B)** RT-PCR analysis of *ASFT* transcripts (1.4 Kb) isolated from roots of wild type and *asft* mutants. **(C)** Genomic organization of the *CYP86B1* gene (At5g23190 locus) in the SALK line SALK_130265 (*cyp86b1*). The T-DNA is inserted into the first exon with left border pointing toward 3' end of the gene (shown as arrow). **(D)** RT-PCR analysis of At5g23190 transcripts isolated from roots of WT and *cyp86b1* mutant line. In **B** and **D**, the *EIF4A1* gene (At3g13920) was used as load control. RB: T-DNA right border, LB: T-DNA left border; LBA1: T-DNA left border specific primer. Genes are shown as arrows; dashed lines within arrows correspond to introns.

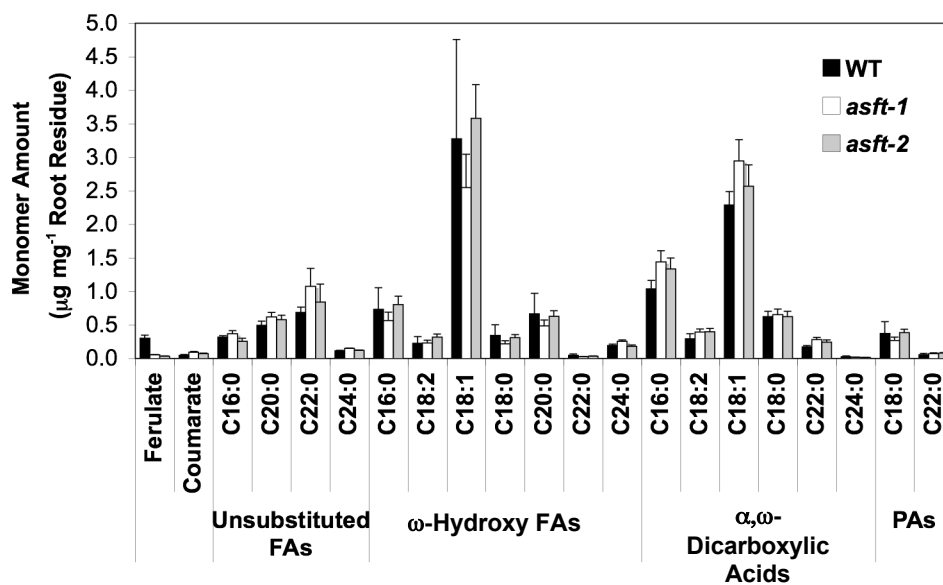


Figure S3: Root suberin monomer composition of WT and *asft* mutants.
 Composition of suberin monomer loads from seven-week old roots. Means of triplicate determinations and SD are indicated.

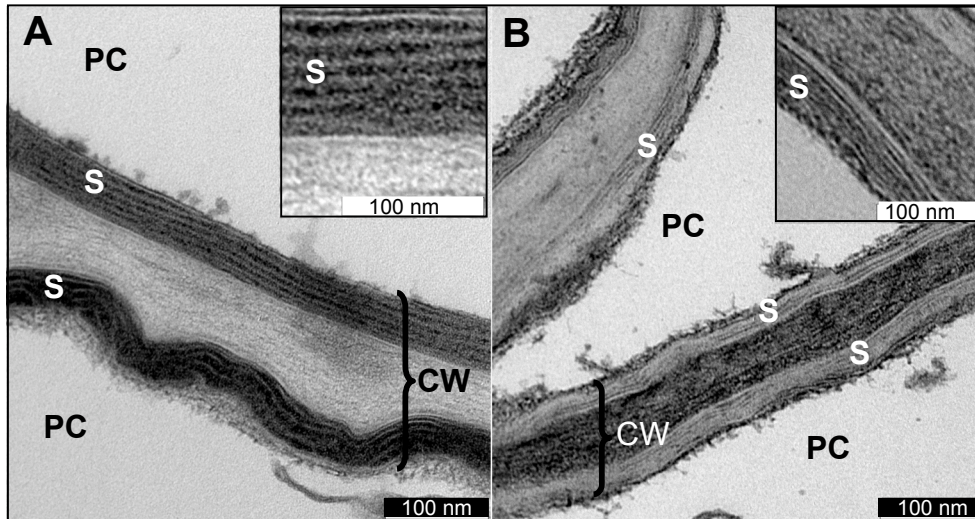


Figure S4: Transmission electron microscopy of suberized peridermal cells in 7-week old roots. Thin samples cut perpendicularly to the suberin lamellae in wild type (**A**) and *cyp86a1* (**B**) root peridermal cells. Samples were stained according to a procedure to enhance the contrast of lipids, as described in Materials and Methods. S: suberin lamellae; CW:cell wall; PC: peridermal cell.

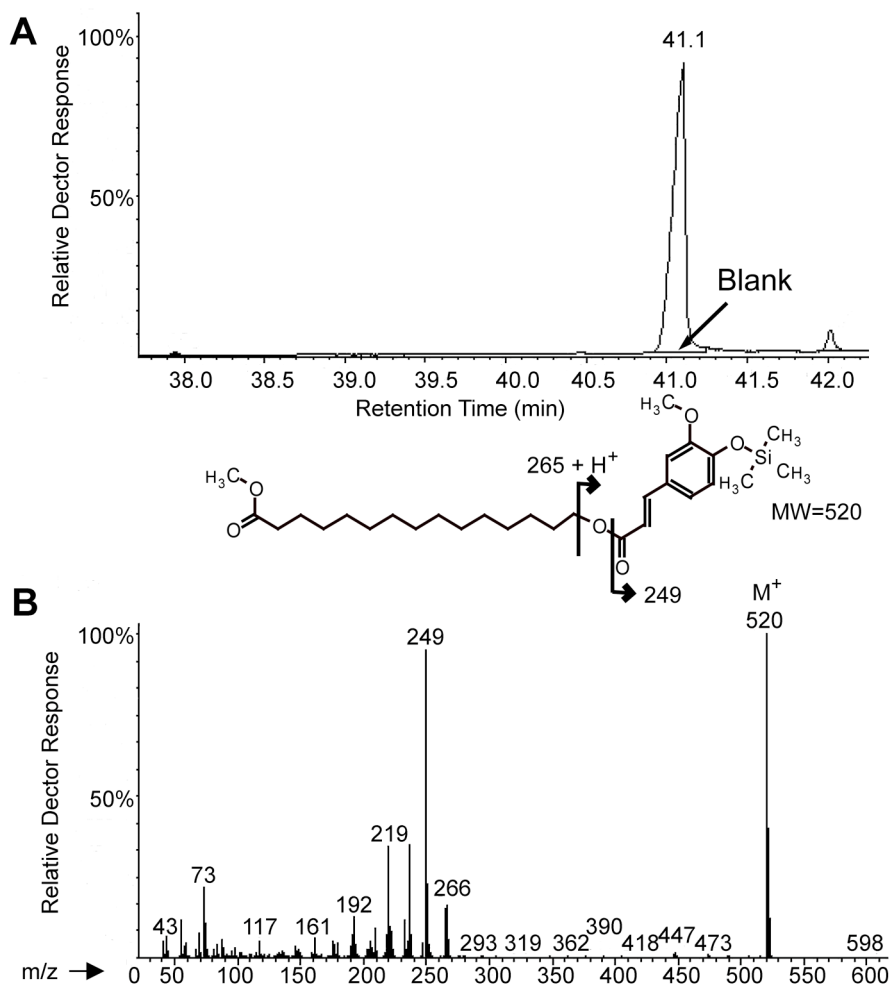


Figure S5: *In vitro* formation of 15-ferulyloxypentadecanoic acid methyl ester by the recombinant ASFT enzyme. (A) The GC-MS partial chromatogram shows a peak at 41 min that is absent if the enzyme is not added (blank). **(B)** EI mass spectrum of ω -O-ferulyloxypentadecanoic acid, methyl ester, trimethylsilyl ether. Diagnostic ions: m/z 520, molecular ion; 266, [TMSi-ferulyloxy + H] $^+$; 265, [TMSi-ferulyloxy] $^+$; 249, [TMSi-feruloyl] $^+$. The molecular structure deduced from the fragmentation pattern is shown on the top of the MS.

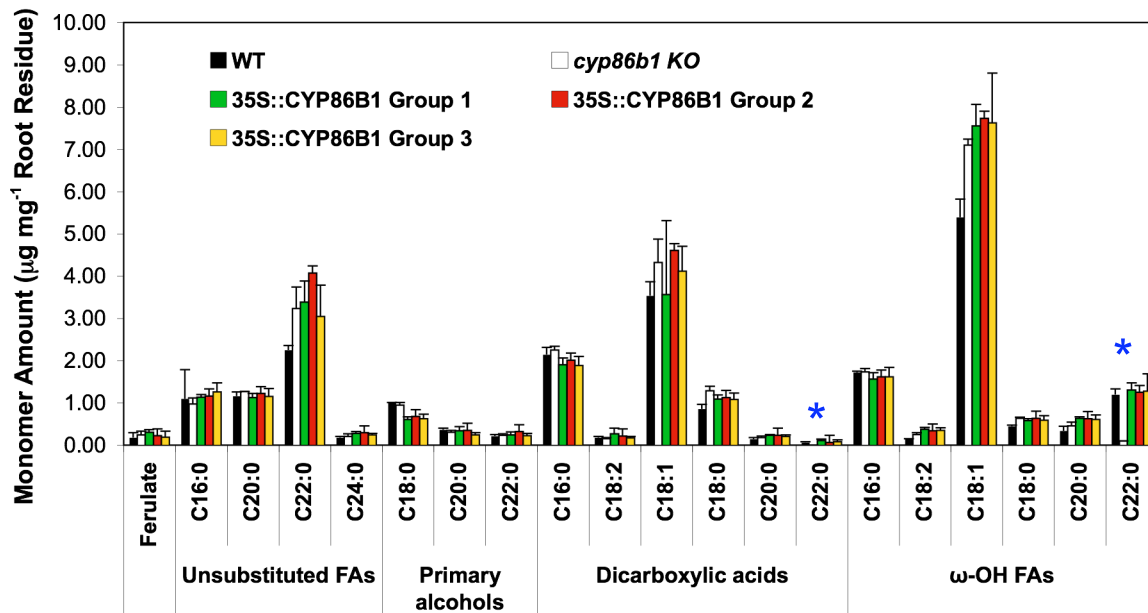


Figure S6: Root suberin monomer composition of WT, *cyp86b1* knockout and the complemented lines 35S::CYP86B1 (6-week-old roots). Eighteen independent lines were screened. Three pools of six lines (“Groups 1, 2, 3”) were analyzed. Means and SD are indicated for each group. Star signs indicate that the mutant was complemented by restoration of the C20 and C22 ω -hydroxy fatty acids, which are absent in the mutant.